## Supplemental Methods:

### Characterization of *ercc-1* worms

All DNA damage sensitivity assays were performed as previously described (Craig et al., 2012)

**A. Embryonic lethality:** Thirty N2 and *ercc-1* synchronized day-1 gravid adults were allowed to lay eggs for 1 h. Eggs were transferred to a fresh NGM plate containing a 1 cm diameter OP50 bacterial lawn in the center of the dish. 48 h later, hatched F1 larvae and unhatched eggs were counted. Embryonic lethality = unhatched eggs/ total eggs counted. Experiments were performed in triplicate.

**B. Higher incidence of males (him) phenotype**: The analysis was performed as described above, except the number of males per population (total larvae) was counted.

**C. Developmental delay**: The analysis was performed as described previously (Lucanic et al., 2011). 24 and 48 h after egg-lay, larvae were imaged on an Olympus IX70 inverted microscope using an Olympus DP70 digital camera. Fiji (Image J) analysis was used to measure the length of each worm.

**D. UV sensitivity assay**: Synchronized N2 and *ercc-1* young adult worms were transferred to NGM plates with no bacteria and exposed to UV radiation at 50, 100 or 250 mJ, or mock irradiated. UV treated worms were allowed to recover on bacteria-containing plates overnight and then transferred to fresh NGM plates for egg lay. 60 eggs were scored for embryonic lethality as described above (A). Experiments were performed in triplicate.

### Stress sensitivity assays in the nematode:

**Stress survival assays**: Plates were prepared 24 h prior to each experiment. All

experiments were performed in triplicate with 40-50 worms. Synchronized N2 and *ercc-1* day 1 adults were exposed to the following stress inducing agents- Rotenone (Sigma-Aldrich, R8875), Antimycin A (Sigma-Aldrich, A8674), Paraquat (Sigma-Aldrich, 36541) at indicated concentration and time. Percent viability is measured as indicated in figure legends.

**Thermotolerance**: Assay performed as previously described (Lithgow et al., 1995). All first day adults were transferred from the growth temperature (20 °C) to a 35 °C heat shock incubator. Percent viability is measured at indicated time points (h).

**Lifespan analysis:** Lifespan analysis was performed as described (Lucanic et al., 2011) with a few changes. Briefly, 40-70 animals were used per condition and viability scored every other day, with or without FUDR. For FUDR lifespans, day 1 adults were transferred to 2.5 $\mu g ml^{-1}$ FUDR-containing NGM plates and were maintained on FUDR for the rest of the lifespan analysis. All lifespan experiments were performed at 20°C unless stated otherwise. Animals that crawled off the plate or were bagged were censored.

**Confocal Microscopy and Image Processing:** Worms were immobilized with 6 mM solution of tetramisole hydrochloride (Sigma) in M9 and mounted on 6% agarose pads on glass slides. Images of worms were acquired using Zeiss LSM 700 upright confocal microscope (Carl Zeiss AG) under nonsaturating exposure conditions. All the images were taken from the same part of *C. elegans*: muscles from the upper part of the worm, excluding the regions of esophagus and vulva. For each condition, multiple worms were imaged. Image processing was performed with the Fiji software (http://imagej.nih.gov/ij; version 1.47b).

**Real-time PCR**: For *C. elegans*: 300 day 1 adult worms were washed three times in S-basal buffer and three replicates were performed as described (Fang et al., 2016). Washed worms were incubated in TRIzol™, dissolved for 20 minutes at 4°C and manufacturers protocol was followed (ThermoFisher Scientific, 15596026). For liver samples: samples were immediately washed in PBS and frozen in RNAlater (Thermo Fisher). Manufacturer's protocol for Trizol RNA isolation was performed. cDNA was generated using Transcriptor First Strand cDNA Synthesis Kit (Roche) and FastStart Universal SYBR Green Master (Rox) was used at a final volume of 20 µL.

**Transcriptome analysis:** The total of 12 Affymetrix mouse 430 V2.0 CEL files (6 WT Control and 6 *Ercc1*$^{-/\Delta}$) were downloaded from the ArrayExpress database with accession number: E-MEXP-1503 (http://www.ebi.ac.uk/arrayexpress/experiments/E-MEXP-1503/samples/). The raw CEL files were processed using Agilent GeneSpring V12.1 (http://www.agilent.com). The Robust Multi-array Average (RMA)/quantile normalization method was used to calculate the signal values for each probe set on these arrays (total of 45101 probe sets on each array). After removing quality control probe sets, a subset of 35423 probe sets with signal higher than 20$^{th}$ percentile in 5 samples or more (at least in one group of replicates) were selected for differential expression analysis. The GeneSpring Volcano Plot function was used to identify differentially expressed probe sets between the WT and *Ercc1*$^{-/\Delta}$ groups. Statistical test parameters were as follows: selected test, Moderated *t*-test; p-value computation, Asymptotic; multiple testing correction, Benjamini- **Hochberg.** The list of probe sets and calculated fold changes and corrected p-values were imported into the Qiagen Ingenuity Pathway Analysis software (http://www.ingenuity.com/). The Ingenuity Core analysis filters were as follows: corrected p-value cut-off was set to 0.05. These filters resulted in selection of 3082 genes for further

analysis. Upstream Analysis output was used to identify FOXO3A targets among these selected genes.

**Generation and culture of primary mouse embryonic fibroblasts (MEFs):** Primary MEFs were generated and cultured as previously reported (Ahmad et al., 2008). In short, MEFs were cultured in a 1:1 mixture of Dulbecco's modified Eagle's medium and Ham's F10 with 10% fetal bovine serum and antibiotics and incubated at 20% oxygen, to induce oxidative stress. Cell lines simultaneously derived from wild-type (WT) littermate embryos were used as controls in all experiments.

**Immunofluorescence:** WT and *Ercc1*$^{-/-}$ MEFs were cultured on 4 well Falcon™ Culture Slides until they reached 60-70% confluence. Cells were fixed with 2% paraformaldehyde in PBS for 10 minutes. Cells were permeabilized and blocked with 5% normal serum / 0.3% Triton™ X-100 in PBS. Antibodies used: TOM20 (CST), FOXO3A (CST, mAb #2497) and Alexa 594-conjugated goat anti-mouse or rabbit IgG (A-11005, Invitrogen, Carlsbad, CA) in PBS with Olympus Confocal microscope.

**Immunoblotting:** Cells were trypsinized, pelleted, and the pellet was dissolved in ice-cold RIPA buffer with Mini-complete protease inhibitor tablet (Roche Applied Science, 11836153001). FOXO3A (Cell Signaling) and tubulin (Abcam, ab4074,) were used at a dilution of 1:1000. This was followed by a 1:5000 dilution of either HRP conjugated anti-rabbit IgG or mouse IgG (Invitrogen).

**Detection of oxidative species with DCFDA:** $H_2$-DCFDA (C6827, Invitrogen, Carlsbad, CA) was used to measure general oxidative stress levels in primary WT and *Ercc1*$^{-/-}$ MEFs. $H_2$-DCFDA (10 mM) in DMSO was diluted in PBS to a final concentration of 10μM in PBS

and added to cells in 10 cm dishes for 20 minutes at 37°C. Following incubation, cells were scraped, pelleted, and resuspended in 1 ml PBS. $H_2$-DCFDA fluorescence intensity was measured on the Cyan LX 9 color high-speed flow cytometer (Beckman Coulter, Brea, CA) and quantified using Summit v.4.3 software.

**Msr enzyme activity assay:** was as described previously (Brunell et al., 2011).

In brief, the reduced product (DABS Met) was separated from the substrate using high-pressure liquid chromatography (HPLC). 250 - 500µg of cell lysate was prepared from tissue samples using a non-detergent method of extraction for the enzymatic assays. The reaction was carried out in the presence of DTT with either dabsyl-methionine–S-sulfoxide, DABS-Met (O)S (for the MsrA assay) or dabsyl-methionine–R-sulfoxide, DABS-Met (O) R (for the MsrB assay) as a substrate.

The reaction mix to measure MsrA activity consisted of 50 mM Tris-Cl (pH7.4),15mM DTT,300 µM DABS- Met (O)S along with mouse liver cell lysate. Samples were incubated at $37^0$C for 30 min and was stopped by adding 300 µl of acetonitrile. Samples were centrifuged at 22,000 rpm for 10 min at 4°C. 20 µl of the supernatant was injected into a C18 HPLC column (Waters, Milford, MA) and the reduced product was detected by absorbance at 436 nm. The enzyme assay was validated by performing time and concentration dependent reactions.

| Gene (mice) | Primer Sequence |
|---|---|
| Sod2- F | 5’-ATGTTGTGTCGGGCGGCG-3’ |
| Sod2-R | 5’-AGGTAGTAAGCGTGCTCCCACACG-3’ |
| Catalase-F | 5′-CCGACCAGGGCATCAAAA-3′ |
| Catalase-R | 5′-GAGGCCATAATCCGGATCTTC-3’ |
| MsrA-F | 5′-TCTGGGTCTTGAAAGGAGTGTA-3’ |
| MsrA-R | 5′-AGGTATTGCTGGTGGTAGTCTTC-3’ |
| Txnrd2-F | 5′-CAGCTTTGTGGATGAGCACACAGTTCG-3 |
| Txnrd2-R | 5′-GATCCTCCCAAGTGACCTGCAGCTGG-3′ |
| | |

**Supplementary Table 1**: List of primers used in mice

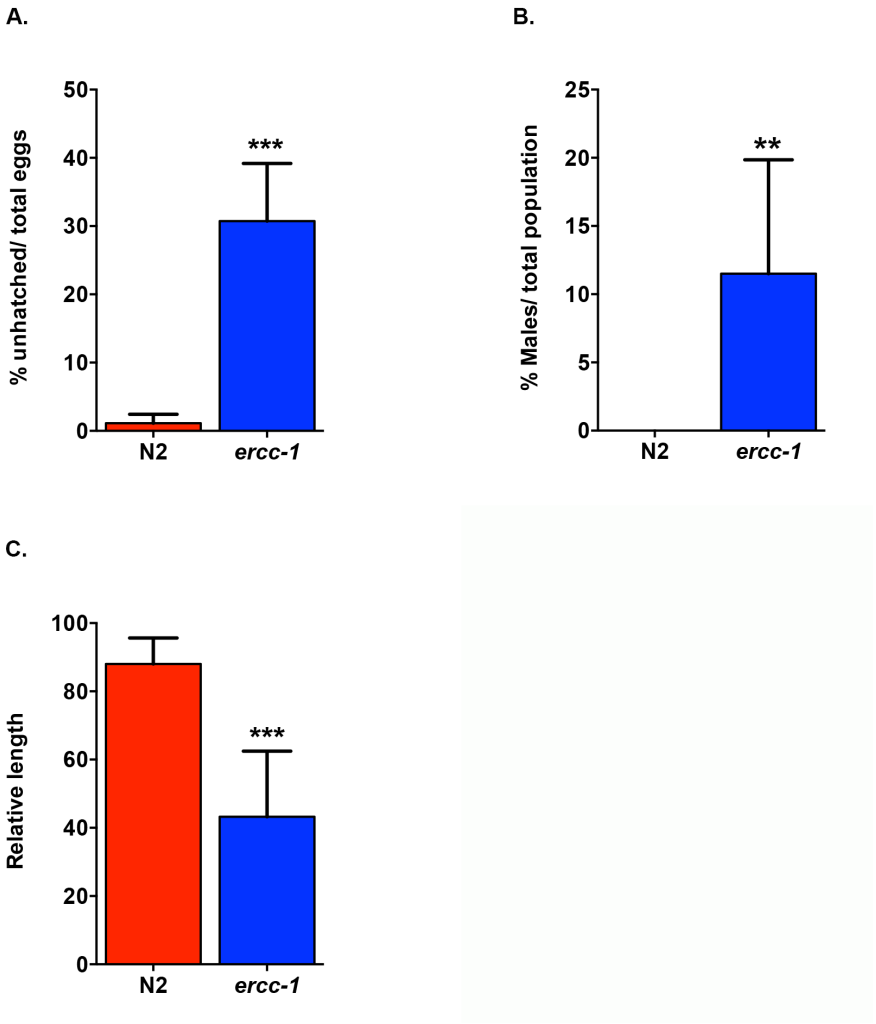


**Figure S1. Loss of *ercc-1* in *C. elegans* leads to genomic instability and growth defects**
**(A)** The percent of unhatched eggs in N2 and *ercc-1* nematodes (mean ± S.D., n = 5 groups of 10-15 worms/ egg lay) ***p<0.001 by Student's one-tailed t-test. **(B)** A higher incidence of males (him) observed in the *ercc-1* mutant worms, indicating increased genome instability (mean ± S.D., n=6 independent population of 50-60 worms) **p<0.01 by Student's one-tailed t-test. **(C)** The development of N2 and *ercc-1* as measured by body length 24 h post-hatching on a group of 15-20 worms. n= 3 independent experiments. ***p<0.001 by Student's one-tailed t-test.

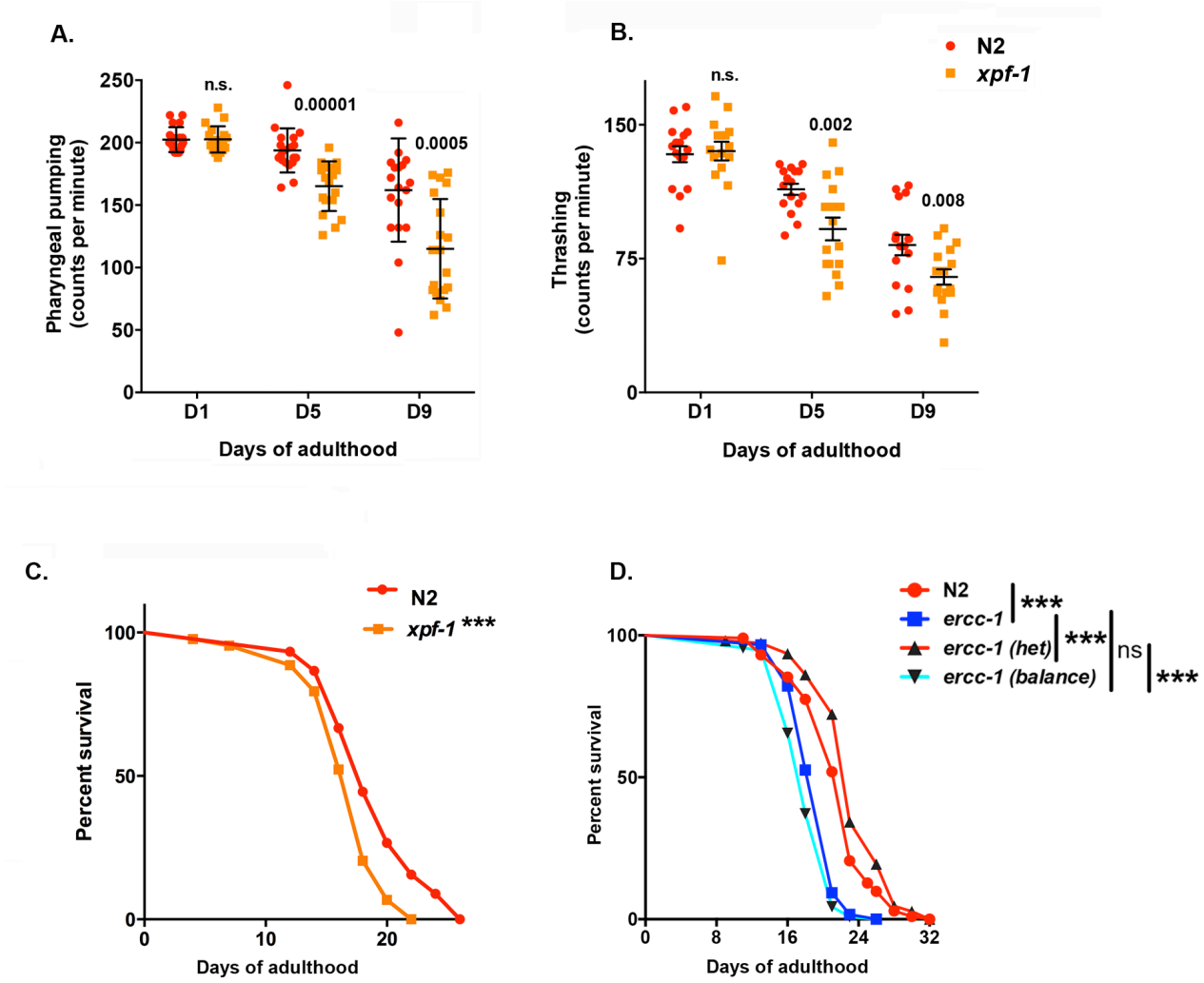


**Figure S2. *ercc-1* phenotypes retained in *xpf-1* mutant worms.**
**(A)** Number of pharyngeal contractions **(B)** Thrashing in liquid per minute for D1, 5 and 9 N2 and *xpf-1* adult worms (mean ± S.E.M., n= 15-20 worms/group; n=3 independent populations) Two-tailed Student's t-test, p values indicated. **(C)** The lifespan of N2 and *xpf-1* mutant worms. Kaplan Meyer survival curves were calculated from populations of 40-70 animals/genotype. Log-rank (Mantel-Cox) test ***p<0.001. **(D)** The lifespan of N2, *ercc-1*, balanced *ercc-1* heterozygotes and *ercc-1* homozygotes derived from the balanced strain. Kaplan Meyer survival curves were calculated from populations of 40-70 animals/genotype. Log-rank (Mantel-Cox) test ***p<0.001, ns not significant

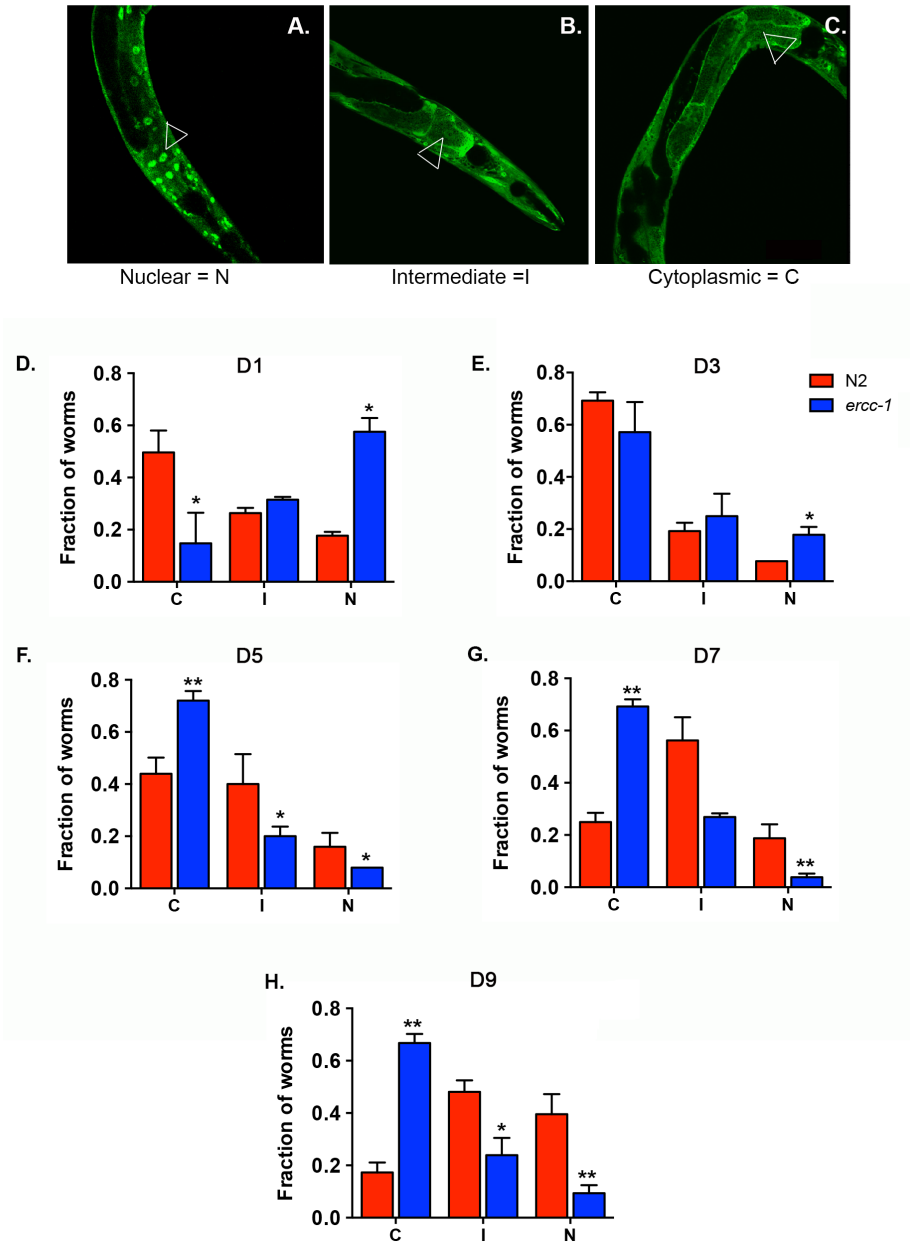


**Figure S3. Altered DAF-16 localization in *ercc-1* worms**
**(A-C)** Representative images of nuclear (N), intermediate (I) and cytoplasmic (C) localization of DAF-16::GFP. **(D-H)** Quantification of DAF16::GFP localization in N2 and *ercc-1* worms of different ages (day= D1,3,5,7,9) graphed as the mean ± S.D. of n = 3 groups of 8-15 worms; Student's one-tailed t-test *$p < 0.05$, **$p < 0.01$.

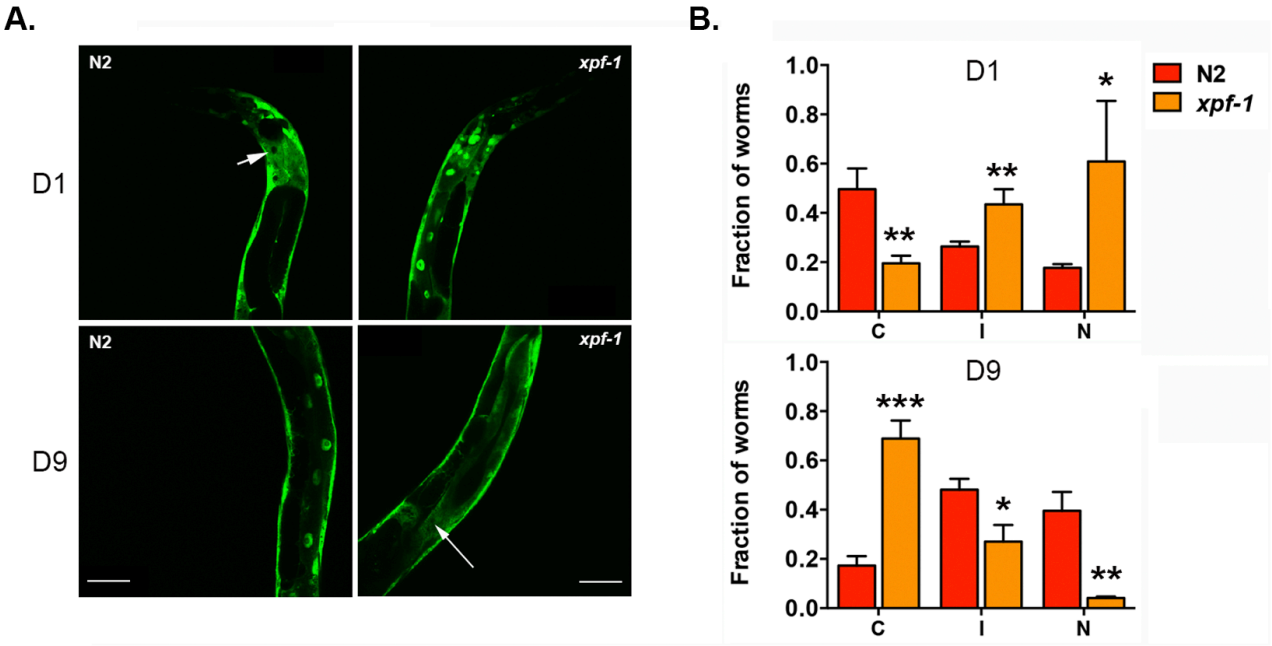


**Figure S4. DAF-16::GFP nuclear localization in *xpf-1* mutant.**
**(A)** Representative images of localization of *daf-16::GFP* in N2 and *xpf-1* adults at day 1 and 9. **(B)** Quantification of DAF-16 localization in N2 and *ercc-1* worms of day1 (top) and 9 (bottom) graphed as the mean ± S.D. of n = 3 groups of 8-15 worms; Student's one tailed t-test *p < 0.05, **p < 0.01, ***p < 0.001.

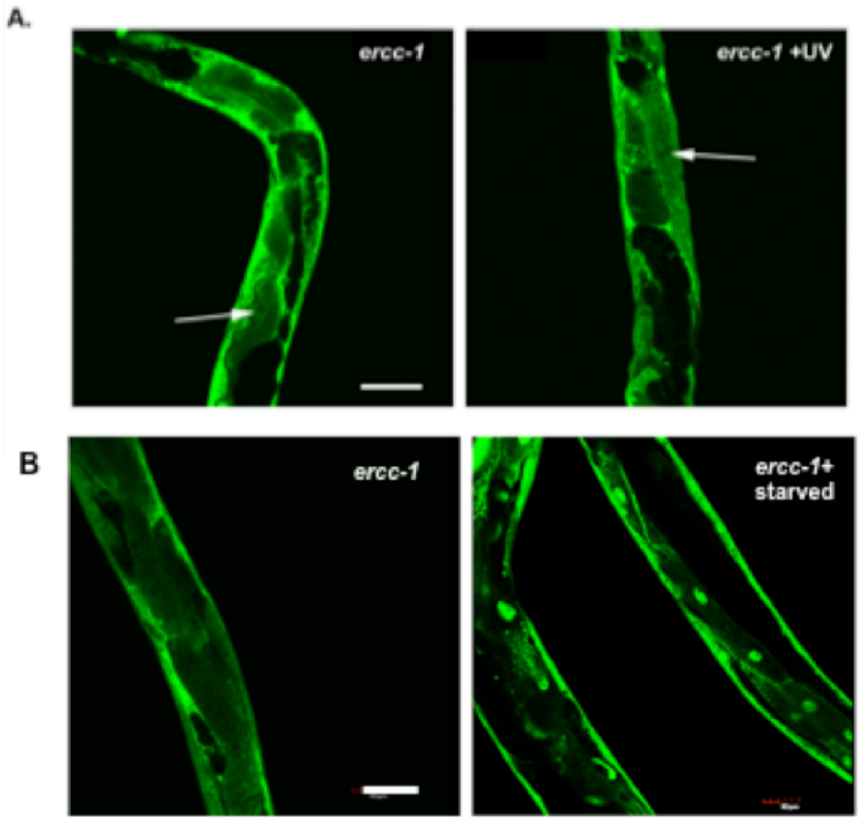


**Figure S5. DAF-16 localization is restored in aged *ercc-1* worms upon starvation but not UV radiation.**
**(A-B)** Representative images of localization of DAF-16::GFP in *ercc-1* worms untreated (left) or treated with **(A)** 40mJ/cm$^2$ UV or **(B)** starvation for 24 h. White arrows indicate lack of DAF-16 in the nucleus.

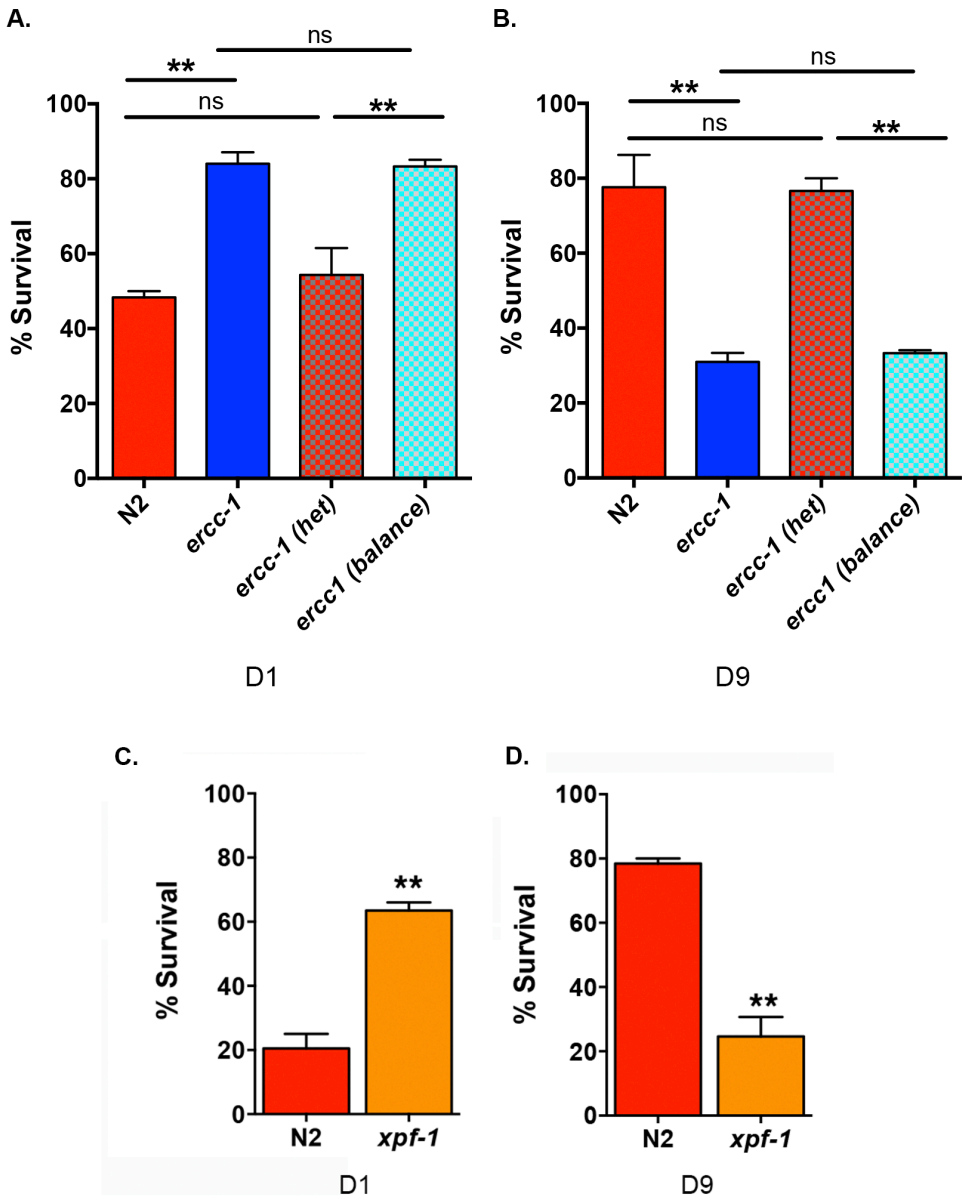


**Figure S6. Temporal dynamics of stress sensitivity in *ercc-1* homozygotes derived from a balanced strain and *xpf-1* mutants.**
**(A-B)** Percent survival of N2, *ercc-1*, balanced *ercc-1* heterozygotes and *ercc-1 (-/-)* homozygotes derived from the balanced strain after treatment with 12.5 µM rotenone for 16 h at day 1 (A) and day 9 (B) of adulthood (mean ± S.E.M., n=4 groups of 40-60 worms). Student's two-tailed t-test **p < 0.01; ns not significant. **(C-D)** Percent survival of N2 and *xpf-1* worms after treatment with 12.5 µM rotenone for 16 h at day 1 and day 9 of adulthood (mean ± S.E.M., n=4 groups of 40-60 worms). Student's two-tailed t-test **p < 0.01.

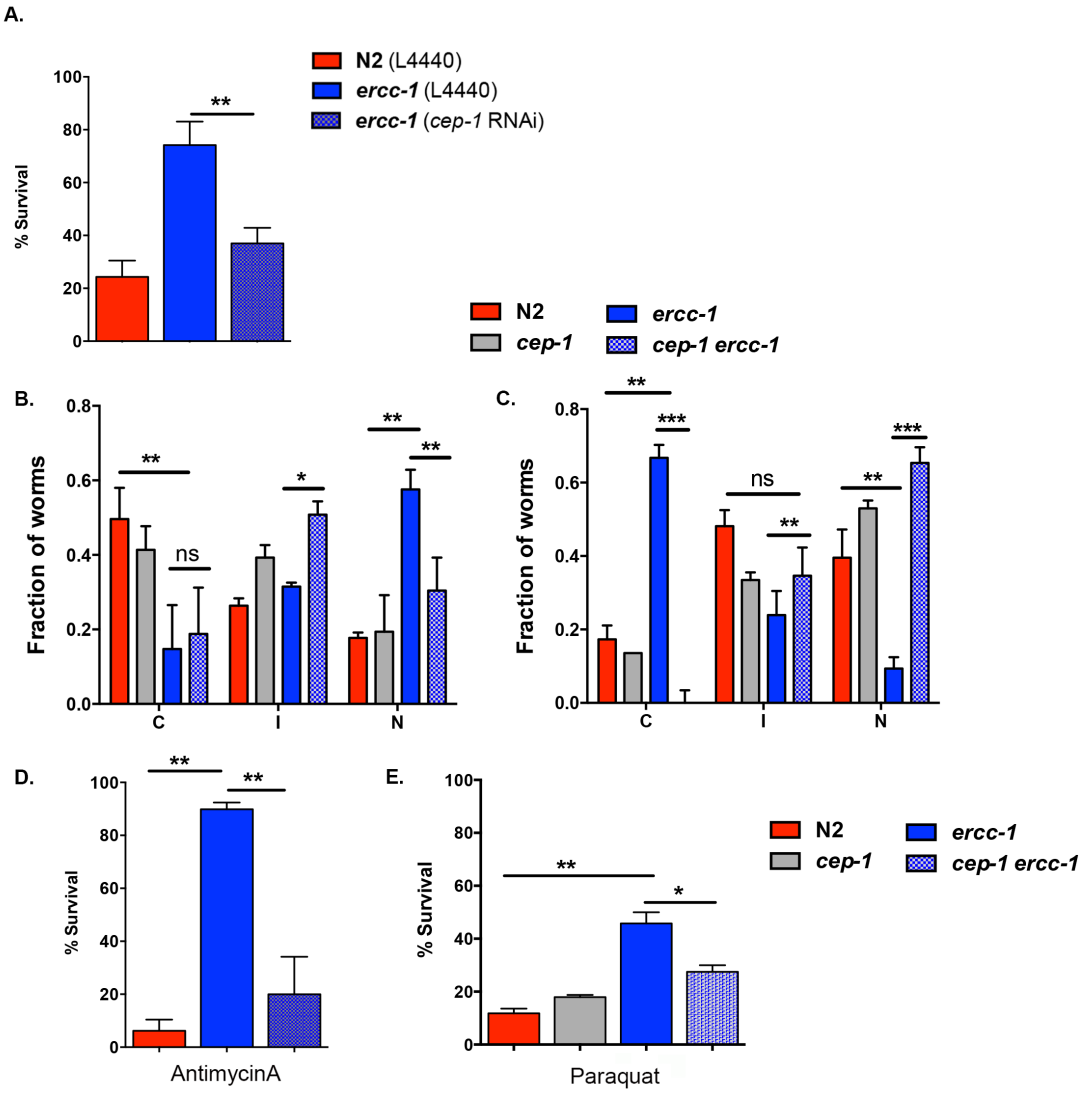


**Figure S7**. **DNA damage response gene, *cep-1* is responsible for DAF-16 dynamics in *ercc-1* worms.**
**(A-B)** Quantification of DAF-16 localization in N2, *cep-1*, *ercc-1* and *cep-1 ercc-1* worms at day 1 **(A)** and day 9 **(B)** nuclear (N), intermediate (I) and cytoplasmic (C) localization of DAF-16::GFP (mean ± S.D. of n = 3 groups of 8-15 worms); Student's one tailed t-test *p < 0.05, **p < 0.01, ***p < 0.001. **(C)** Percent survival of N2, *ercc-1* and *cep-1 ercc-1* worms after treatment with 25 µM antimycin A for 12 h (mean ± S.E.M., n=3 groups of 40-60 worms). Student's two-tailed *t-test* **p< 0.01. **(D)** Viability of N2, *cep-1*, *ercc-1* and *cep-1 ercc-1* day 1 adult worms after treatment with 100 mM paraquat for 12 h (mean ± S.E.M., n=4 groups of 40-60 worms). Student's two-tailed *t-test* *p< 0.05 and **p < 0.01.

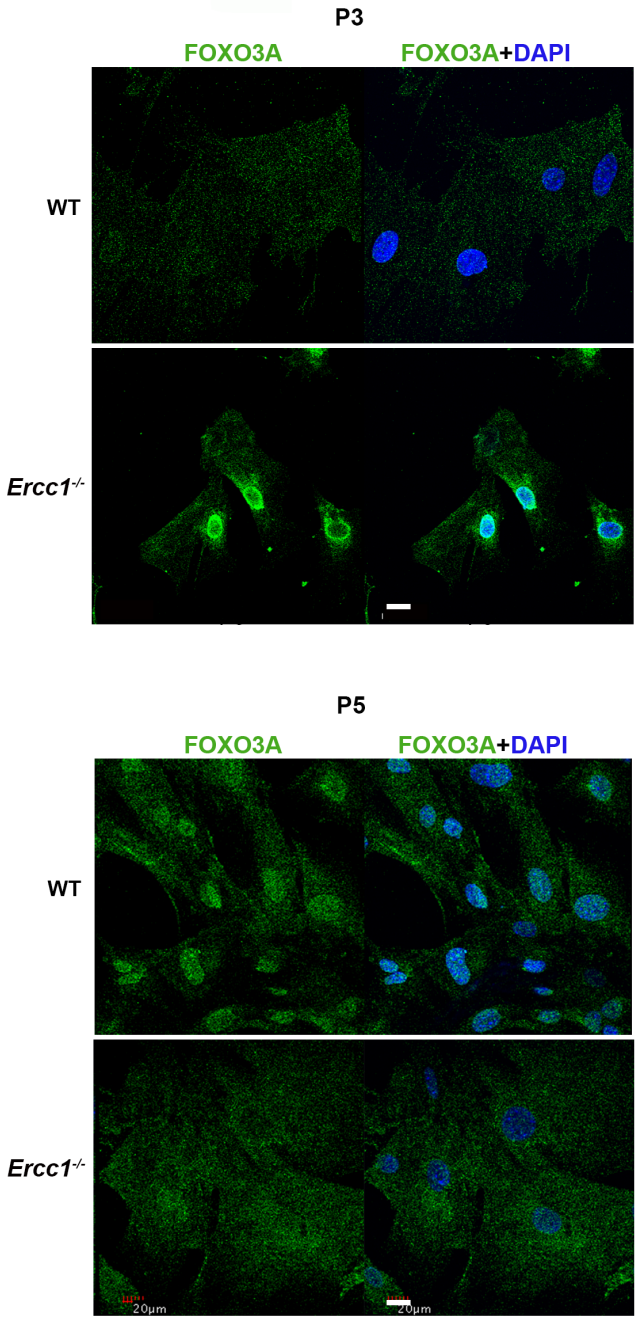


**Figure S8. Altered FOXO3A subcellular localization in *Ercc1*$^{-/-}$ MEFs**
Immunofluorescence detection of FOXO3A in WT and *Ercc1*$^{-/-}$ primary MEFs at early (P3, top) and late (P5, bottom) passages. Nuclei are stained with DAPI. Scale bar = 20μm.

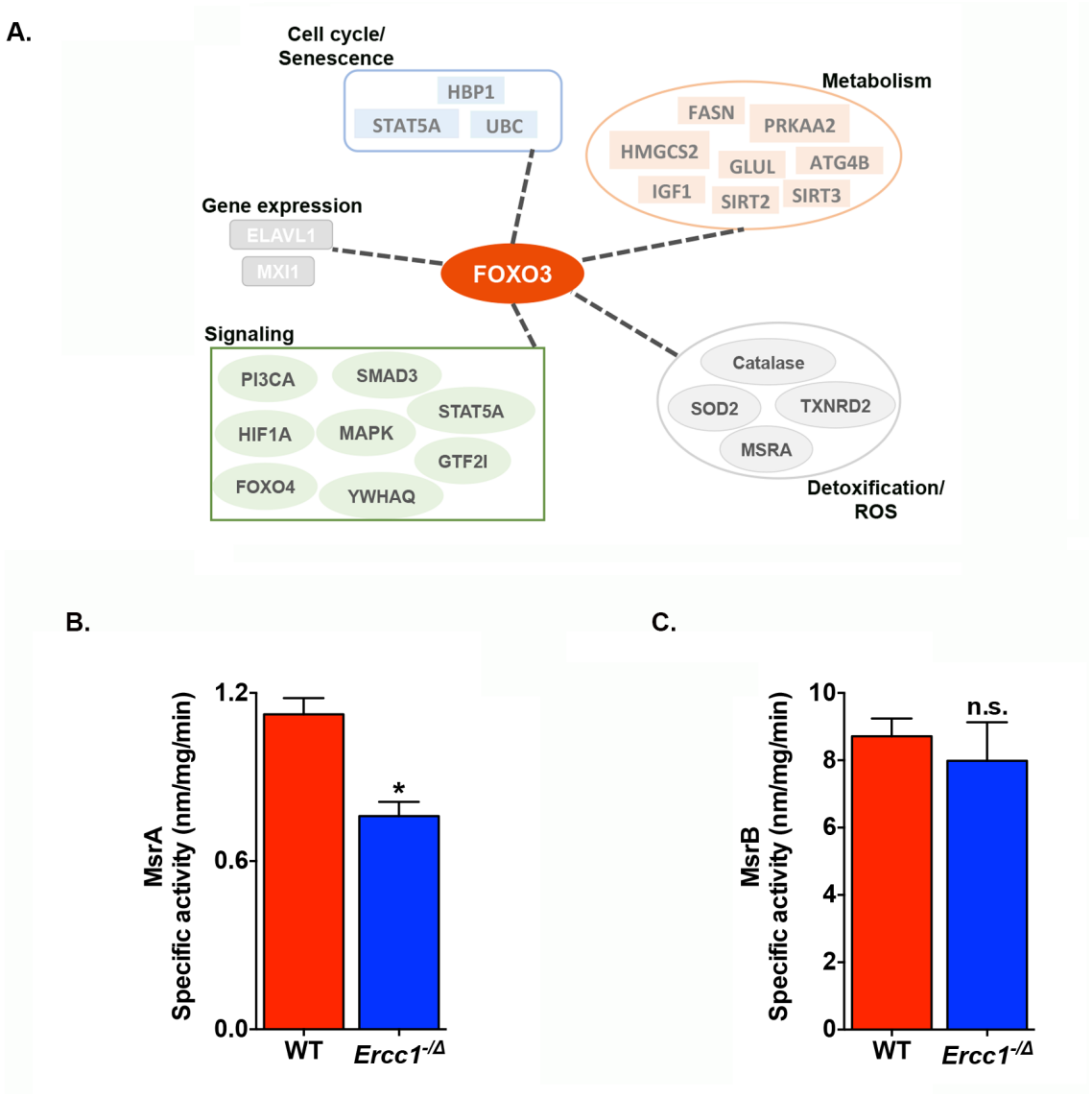


**Figure S9**. **FOXO3A activity is reduced in DNA repair-deficient *Ercc1*$^{-/\Delta}$ mice**
**(A)** Analysis of the gene expression data in liver from 16 week-old *Ercc1*$^{-/\Delta}$ mice and wild-type littermates using Ingenuity Pathway Analysis (IPA) software. The schematic diagram depicts targets of FOXO3A that were significantly downregulated in *Ercc1*$^{-/\Delta}$ mice compared to age-matched WT controls. **(B)** MsrA enzymatic activity tested in 16 week-old livers from WT and *Ercc1*$^{-/\Delta}$. **(C)** MsrB enzymatic activity tested in 16 week-old livers for age-matched WT and *Ercc1*$^{-/\Delta}$. Student's one tailed t-test *$p < 0.05$, ns is not significant

**Table 2**: Summary of lifespan experiments with *C. elegans* strains

| Trial | Genotype | Median survival | Deaths (censored) | P value *vs* N2 |
|---|---|---|---|---|
| Trial 1 | N2 | 17.5 | 69(0) | |
| | *ercc-1* | 15 | 71(0) | <0.0001 |
| Trial 2 | N2 | 22 | 40(5) | |
| | *ercc-1* | 16.5 | 49(2) | <0.0001 |
| Trial 3 | N2 | 17.8 | 59(0) | |
| | *ercc-1* | 13.9 | 70(4) | <0.0001 |
| Trial 1 | N2 (no FUDR) | 17.2 | 45(2) | |
| | *ercc-1*(no FUDR)* | 15.8 | 55(5) | 0.0117 |
| Trial 2 | N2 (no FUDR) | 16 | 52(0) | |
| | *ercc-1*(no FUDR)* | 13 | 55(0) | 0.0279 |
| Trial 1 | N2 | 23.75 | 52(2) | |
| | *ercc-1** | 18.83 | 60(1) | <0.0001 |
| | *ercc-1 (het)** | 22.98 | 61(1) | 0.1281 |
| | *ercc-1(-/-)** | 17.45 | 55(2) | <0.0001 |
| Trial 2 | N2 | 23.8 | 50(1) | |
| | *ercc-1** | 18.68 | 58(0) | <0.0001 |
| | *ercc-1 (het)** | 23.08 | 45(2) | 0.162 |
| | *ercc-1(-/-)** | 17.98 | 59(1) | <0.0001 |
| Trial 3 | *ercc-1 (het)** | 23.34 | 52(0) | |
| | *ercc-1(-/-)** | 19.6 | 52(0) | <0.0001** |
| Trial 1 | N2 | 14.9 | 141 | |
| | *xpf-1** | 11 | 159 | <0.0001 |
| Trial 2 | N2 | 17.2 | 45(0) | |
| | *xpf-1** | 15.6 | 44(0) | 0.0035 |
| Trial 3 | N2 | 17.5 | 45(0) | |
| | *xpf-1** | 15.9 | 27(0) | 0.0452 |

*Backcrossed strains
**P value vs *ercc-1 (het)*
*ercc-1(-/-)* homozygous mutant progeny from a genetically balanced *ercc-1* strain

**References:**

1. Craig AL, Moser SC, Bailly AP, & Gartner A (2012) Methods for studying the DNA damage response in the Caenorhabdatis elegans germ line. Methods Cell Biol 107:321-352.

2. Lucanic M, et al. (2011) N-acylethanolamine signalling mediates the effect of diet on lifespan in Caenorhabditis elegans. Nature 473(7346):226-229.

3. Lithgow GJ, White TM, Melov S, & Johnson TE (1995) Thermotolerance and extended life-span conferred by single-gene mutations and induced by thermal stress. Proc Natl Acad Sci U S A 92(16):7540-7544.

4. Fang EF, et al. (2016) NAD+ Replenishment Improves Lifespan and Healthspan in Ataxia Telangiectasia Models via Mitophagy and DNA Repair. Cell Metab 24(4):566-581.

5. Mouchiroud L, et al. (2013) The NAD(+)/Sirtuin Pathway Modulates Longevity through Activation of Mitochondrial UPR and FOXO Signaling. Cell 154(2):430-441.

6. Wu JJ, et al. (2009) Mitochondrial dysfunction and oxidative stress mediate the physiological impairment induced by the disruption of autophagy. Aging (Albany NY) 1(4):425-437.

7. Lavasani M, et al. (2012) Muscle-derived stem/progenitor cell dysfunction limits healthspan and lifespan in a murine progeria model. Nat Commun 3:608.

8. Brunell D, Sagher D, Kesaraju S, Brot N, & Weissbach H (2011) Studies on the metabolism and biological activity of the epimers of sulindac. Drug Metab Dispos 39(6):1014-1021.